

Expansion of Ultracold Neutral Plasmas with Exponentially Decaying Density Distributions

M. K. Warrens,¹ G. M. Gorman,¹ S. J. Bradshaw,¹ and T. C. Killian¹
Rice University, 6100 Main St. Houston, TX, 77005

(Dated: 1 January 2021)

We present a study of the expansion of an ultracold neutral plasma (UCNP) with an initial density distribution that decays exponentially in space, created by photoionizing atoms shortly after their release from a quadrupole (or biconic cusp) magnetic trap. A characteristic ion acoustic timescale is evident in the evolution of the plasma size and velocity, indicating the dynamics are reasonably well described by a model of hydrodynamic expansion of a quasi-neutral plasma. However, for low plasma density and high initial electron temperature, excess ion kinetic energy in the vicinity of the central density peak suggests significant local non-neutrality at early times. Observations are compared to the well-understood self-similar expansion of an UCNP with an initial Gaussian density distribution, and a similar scaling law describes the evolution of plasma size for both cases.

I. INTRODUCTION

Expansion of plasma into surrounding vacuum is a common phenomenon in many situations, such as astrophysical^{1,2} and solar plasmas,^{3–5} and plasmas created by intense laser-matter interaction.^{6–15} Depending upon plasma length scales and particle velocities, complex phenomena can arise reflecting hydrodynamic and kinetic effects, collective modes, and instabilities. Here, we investigate the expansion of an unmagnetized ultracold neutral plasma (UCNP) with an initial density distribution that is sharply peaked and decays exponentially with increasing distance from the plasma center.

Expansion of an UCNP with a spherical Gaussian density distribution is well-studied^{16–19} and known to be self-similar and predominantly hydrodynamic. The sharply peaked density profile of the exponentially decaying distribution raises questions about the validity of a hydrodynamic description in this case. Understanding the dynamics for this new plasma shape is important because ongoing experiments studying magnetized UCNPs in biconic cusp magnetic fields²⁰ typically start with a plasma with an exponentially decaying density distribution. In order to identify the influence of magnetic forces, it is beneficial to understand the unmagnetized case.

II. UCNPS

UCNPs^{21–23} are formed by photo-exciting laser cooled atoms²⁴ or molecules in a supersonic expansion²⁵ near the ionization threshold, yielding ion temperatures below 1 K, electron temperatures ranging from 1 – 1000 K, and densities ranging from $10^6 - 10^{12} \text{ cm}^{-3}$. Such systems have shed light on equilibration^{26–39} and transport⁴⁰ in strongly coupled plasmas,⁴¹ which has connections to laser-produced plasmas^{32,42} extending into the warm-dense-matter and high-energy-density regimes.^{43,44} With excellent control over the initial conditions and precise diagnostics, they have been used to benchmark theories and numerical techniques for quantum,⁴⁵ molecular-dynamic,^{38,40} kinetic,³⁴ and hydrodynamic descriptions,^{46,47} and to observe and characterize collective modes and instabilities.^{16,48–50} UCNPs are also being developed for applications in bright ion and electron

beams.^{51–56} UCNPs created from molecules display additional processes such as dissociative recombination⁵⁷ and arrested relaxation.⁵⁸

For the experiments discussed here, UCNPs are formed by direct photoionization of laser-cooled Sr atoms.^{26,59} After photoionization, an UCNP undergoes several stages of equilibration and expansion. The first stage is electron equilibration on the timescale of an electron plasma oscillation. Direct ionization yields a well-defined electron thermal energy given by the energy excess of the ionizing laser above the ionization threshold.²¹ For low electron energy or high density, heating processes such as disorder-induced heating and three-body recombination^{60,61} may increase the electron temperature.^{17,29,62} This regime is avoided in the experiments described here. During electron equilibration, some of the electrons escape, creating a potential energy well that traps the remaining electrons.²¹ The second stage of the UCNP evolution is ion equilibration, which occurs on the timescale of an ion plasma oscillation, which is $\sim 1 \mu\text{s}$ for typical UCNP densities. Disorder-induced heating causes the ion temperature to increase as the initially uncorrelated ions develop spatial correlations and convert excess potential energy to kinetic energy.^{28,36} The final stage of the UCNP evolution is expansion into surrounding vacuum.^{19,63}

The plasma expansion depends critically upon the plasma's initial density distribution, which follows the density profile of the neutral atoms just before photoionization. For UCNPs created from laser-cooled atoms, atoms are typically photoionized after release from a magneto-optical trap (MOT), a trap formed by near-resonant light scattering in the presence of spatially varying Zeeman shifts of the optical transition.^{24,64} This results in a Gaussian density distribution of

$$n(\vec{r}) = n_0 \exp \left[-\frac{x^2}{2\sigma_x^2} - \frac{y^2}{2\sigma_y^2} - \frac{z^2}{2\sigma_z^2} \right]. \quad (1)$$

An alternative scheme is to trap atoms in a purely magnetic trap before photoionization. Such a trap is formed by the conservative potential $U = -\vec{\mu} \cdot \vec{B}$ arising from the interaction of an atom's magnetic moment $\vec{\mu}$ with the magnetic field \vec{B} .²⁴ Magnetic trapping is readily available for Sr atoms,⁶⁵ and as

described in Sec. III, the particular field geometry used for Sr UCNP experiments results in a cylindrically symmetric, exponentially decaying density for the atomic cloud and plasma,

$$n(\vec{r}) = n_0 \exp \left[-\frac{\sqrt{x^2 + (y^2 + z^2)/4\eta^2}}{\alpha} \right]. \quad (2)$$

$\eta = 1$ for an atomic sample in thermal equilibrium, but we allow for this parameter to vary as an additional degree of freedom when analyzing data.

For the rest of the paper, we will refer to plasmas with Gaussian (Eq. 1) and exponentially decaying (Eq. 2) initial density distributions as Gaussian plasmas and exponential plasmas respectively.

III. EXPERIMENTAL METHODS

A. Details of Sr Ultracold Neutral Plasma Creation

To form Gaussian UCNPs, Sr atoms are first laser-cooled and trapped in a MOT using the $1S_0 - 1P_1$ transition at 461 nm (Fig. 1). The MOT is then extinguished and atoms in the $5s^2 1S_0$ ground state are photoionized using overlapping 10 ns pulses of 461 nm and ~ 412 nm light.²⁶

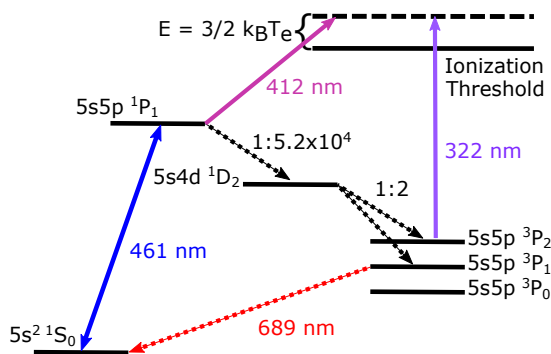


FIG. 1. Levels and transitions for laser cooling of strontium atoms and subsequent photoionization to form an UCNP.

To form exponential UCNPs, atoms are initially laser-cooled and trapped in the MOT. During laser cooling, atoms naturally populate the $5s5p^3P_2$ state due to a small branching ratio for decay from the upper state ($5s5p^1P_1$) through the $5s4d^1D_2$ state into the $5s5p^3P_2$ state, where low field seeking atoms are trapped by the quadrupole (or biconic cusp) magnetic field of the MOT because of the large magnetic moment of $5s5p^3P_2$ atoms.⁶⁵ The density distribution of the magnetically trapped neutral atoms is well approximated by Eq. 2. After loading the magnetic trap for a variable time ~ 1 s, the magnetic field and laser-cooling light are turned off. After a delay of 280 μ s to allow eddy currents in the vacuum chamber to decay, 3P_2 atoms are photoionized with a 10 ns, 10 mJ pulse of ~ 322 nm light. This delay time is short compared to the timescale for appreciable motion of the atoms, and the ionizing beam is approximately uniform over the spatial ex-

tent of the atom cloud. By varying the loading time, the initial plasma density is varied from $1 - 40 \times 10^8 \text{ cm}^{-3}$.

The characteristic size of the exponentially decaying plasma is $\alpha = 3k_B T / 8\mu_B B' \approx 1$ mm, where $T \approx 2$ mK is the temperature of the precursor neutral atoms, and $B' = 150$ G/cm is the gradient of the magnetic field along the symmetry axis (\hat{x}). μ_B and k_B are the Bohr magneton and Boltzmann constant respectively. The atom cloud is small compared to the radius of the coils creating the magnetic field, so a linear approximation of the field profile is sufficient.

B. Imaging an Ultracold Neutral Plasma

We image ions in an UCNP using laser-induced fluorescence (LIF).⁶⁶ A 1 mm thick sheet of 422 nm light passes through the center of the plasma and along the symmetry axis of the coils generating the MOT magnetic field. This light drives the $5s^2S_{1/2} - 5s^2P_{1/2}$ Sr^+ transition, and emitted fluorescence is imaged onto an intensified CCD camera along a direction (\hat{z}) perpendicular to the laser sheet. Varying the detuning of the imaging beam yields a spatially resolved LIF spectrum. Local ion temperature and velocity are extracted from a fit of the spectrum to a Voigt profile. We image the plasma for 500 ns, which is short compared to the expansion time of the UCNP. Times reported are from the middle of the imaging window. Density maps of the central plane of the plasma are created by integrating the local spectra over frequency. The proportionality between LIF intensity and density is calibrated using disorder-induced heating curves as an absolute measure of density.⁶⁷ The LIF optical configuration does not provide information on the z -dependence of the density distribution. In the analysis, we assume cylindrical symmetry about the x -axis, reflecting the magnetic field symmetry.

Figure 2 shows false-color images and transects of the density for an exponential plasma with initial peak density $3.2 \times 10^9 \text{ cm}^{-3}$ and $T_e(0) = 160$ K and a Gaussian plasma with initial peak density $1.2 \times 10^9 \text{ cm}^{-3}$ and $T_e(0) = 40$ K shortly after photoionization. The fit function for the exponential plasma (Fig. 2) is obtained by integrating Eq. 2 over the width of the imaging sheet, and α , η and n_0 are varied to match the data. We find $\eta = 0.83$, close to the expected value.

Deviations between the data and fit most likely result from non-uniformities in the photoionization beam, lack of thermal equilibrium of atoms in the magnetic trap, and plasma evolution during the short delay between photoionization and LIF imaging. In spite of these imperfections, from the comparison of the Gaussian and exponential data in Fig. 2, it is clear that the exponential plasma is much more sharply peaked than the Gaussian plasma.

IV. PLASMA EXPANSION

Hydrodynamic models accurately describe the evolution of plasma density in collisional systems, for which the length scales of plasma inhomogeneities are much larger than the

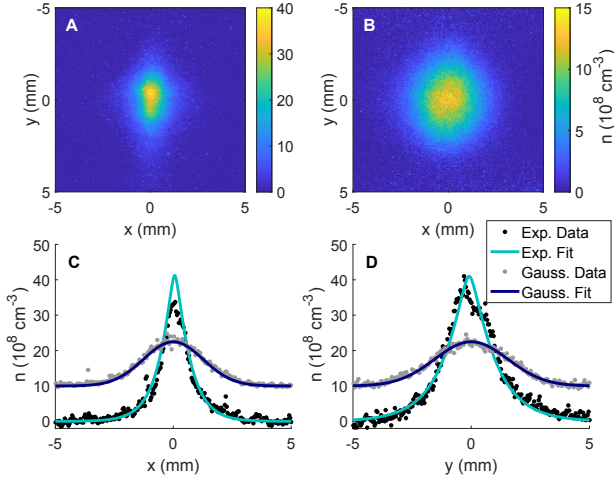


FIG. 2. (A) False-color image of the density profile at $t = 350$ ns after photoionization for an exponential plasma with $T_e(0) = 160$ K. (B) Density profile at $t = 330$ ns for a Gaussian plasma with $T_e(0) = 40$ K. (C) X-transect through the center of the plasmas shown in (A) and (B). (D) Y-transect through the center of the plasmas shown in (A) and (B). Fit lines in (C) and (D) are integrals over LIF-laser-sheet thickness of Eq. 1 for the Gaussian plasma and of Eq. 2 for the exponential plasma.

particle mean free path and the particles are close to local thermal equilibrium.^{46,47} Assuming quasineutrality²² ($n_e \approx n_i \equiv n$ for electron and ion densities n_e and n_i) and the absence of any magnetic forces, this implies the following equation for the rate of change of the local hydrodynamic velocity \vec{u} in the limit of $T_i \ll T_e$

$$m_i \dot{\vec{u}} \approx -k_B T_e \frac{\vec{\nabla} n}{n}, \quad (3)$$

where m_i is the ion mass, k_B is the Boltzmann constant, and T_e and T_i are the electron and ion temperatures respectively. Eq. 3 describes a hydrodynamic expansion driven by the electron pressure gradient.

A. Self-similar Expansion of an UCNP with a Spherical Gaussian Density Distribution

For Gaussian UCNPs, a hydrodynamic description in terms of coupled equations for electrons and ions captures the dominant behavior of UCNP expansion.^{16,19,22} Various authors have shown that a hydrodynamic treatment neglecting ion-electron thermalization⁶⁸ and inelastic processes^{60,62,69} predicts that a Gaussian UCNP undergoes self-similar expansion, described by Eq. 1 with $\sigma \rightarrow \sigma(t)$.^{17,22,34} A comprehensive treatment,^{22,34} deriving the evolution of hydrodynamic moments from kinetic equations, yields the following equations describing the evolution of plasma density and constituent temperatures,

$$\sigma^2(t) = \sigma^2(0) \left(1 + t^2/\tau_{\text{exp}}^2\right), \quad (4)$$

$$\gamma(t) = \frac{t/\tau_{\text{exp}}^2}{1 + t^2/\tau_{\text{exp}}^2}, \quad (5)$$

$$T_i(t) = \frac{T_i(0)}{1 + t^2/\tau_{\text{exp}}^2}, \quad (6)$$

$$T_e(t) = \frac{T_e(0)}{1 + t^2/\tau_{\text{exp}}^2}, \quad (7)$$

The characteristic plasma expansion time is given by

$$\tau_{\text{exp}} = \sqrt{\frac{m_i \sigma(0)^2}{k_B [T_e(0) + T_i(0)]}} \approx \sqrt{\frac{m_i \sigma(0)^2}{k_B T_e(0)}} \quad (8)$$

and the hydrodynamic expansion velocity follows

$$\mathbf{u}(\mathbf{r}, t) = \gamma(t) \mathbf{r}. \quad (9)$$

Equations 3 and 9 both yield the acceleration $\dot{\vec{u}} \approx \frac{k_B T_e(t)}{m_i \sigma(t)^2} \vec{r}$. The linear dependence of the velocity and acceleration upon displacement vector \vec{r} ensures the self-similarity of the expansion. Experiments confirm that the analytic solution describes the expansion of a Gaussian UCNP extremely well.¹⁹

B. Expansion of an UCNP with an Exponentially Decaying Density Distribution

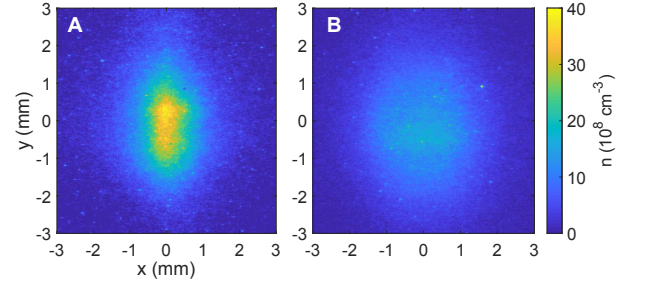


FIG. 3. False color images showing expansion of an exponential plasma with initial peak density $4.4 \times 10^9 \text{ cm}^{-3}$ and $T_e(0) = 40$ K. (A) $t = 350$ ns after plasma creation. (B) $t = 11 \mu\text{s}$ after plasma creation.

For an exponential plasma (Eq. 2), the length scale for density variation is $|n/\vec{\nabla} n| \sim \alpha \sim 1$ mm. The ion mean-free path is typically several orders of magnitude smaller than this, and the electron mean-free path is typically similar to or smaller than α for most of the plasma over the range of accessible UCNP conditions. In addition, electrons rapidly thermalize with small Debye screening length in the self-consistent potential of the ions and electrons. This suggests that hydrodynamic models should describe the expansion well, as observed in previous experiments with Gaussian plasmas,^{19,46} except perhaps very near the center of the plasma where the density gradient is not well defined.

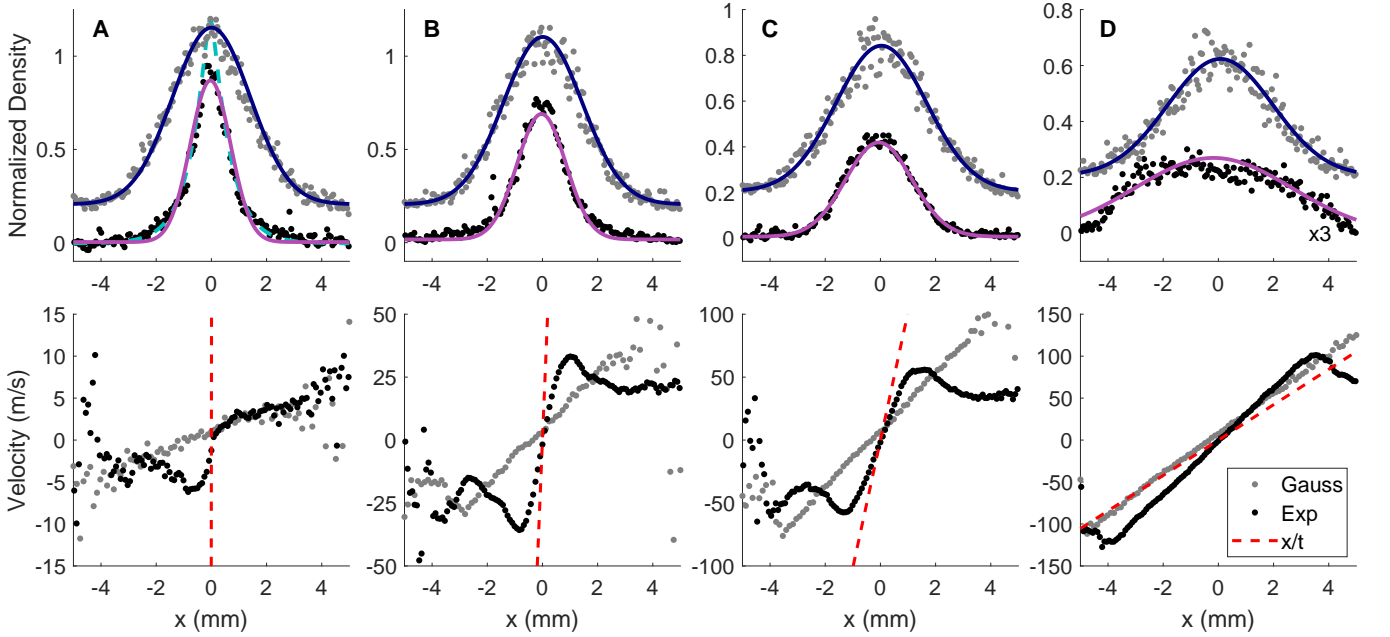


FIG. 4. Transects along the x -axis of the plasma density distribution (top) and velocity (bottom), for Gaussian and exponential plasmas for initial peak densities of $1.0 \times 10^9 \text{ cm}^{-3}$ and $3.5 \times 10^9 \text{ cm}^{-3}$ respectively and electron temperature $T_e(0) = 40 \text{ K}$. Density transects for the Gaussian plasmas are offset for clarity. The time after photoionization is (A) $0.34 \pm 0.01 \mu\text{s}$, (B) $5.7 \pm 0.1 \mu\text{s}$, (C) $14 \pm 4 \mu\text{s}$, and (D) $27 \pm 3 \mu\text{s}$. All density transects are fit to integrals over LIF-laser-sheet thickness of Eq. 1 (solid lines). The first time point (A) for the exponential plasma is also fit to the integral over LIF-laser-sheet thickness of Eq. 2 (dashed line).

A first indication of the hydrodynamic nature of expansion of an exponential UCNP is given by the false-color images of the density (Fig. 3). The rapid expansion along the initially narrow axis of the plasma is a characteristic signature of hydrodynamic behavior in which the acceleration is proportional to the local density gradient (Eq. 3).

To go beyond this qualitative conclusion, we look quantitatively at the evolution of the plasma size. Figure 4(top) shows transects of the evolving density distributions for Gaussian and exponential plasmas with initial electron temperature of $T_e(0) = 40 \text{ K}$. The transects pass through the plasma center along the initially smaller dimension of the exponential plasma (along the x -axis). Density is normalized by the initial peak density. The Gaussian plasma remains Gaussian as predicted for the self-similar expansion (Eqs. 4-7).¹⁹ The transects for the exponential plasma show that the plasma is initially exponential, but does not expand self-similarly. The density first decreases at the center, rounding out the sharp peak and causing the density distribution to approach a Gaussian. However, it does not retain the Gaussian shape, and the gradient steepens along the advancing edges of the plasma, suggestive of wave breaking.^{13,18}

To quantitatively describe the plasma expansion, we extract characteristic sizes with numeric fits to the data (Fig. 4(top)). The exponential (Eq. 2), integrated over the LIF laser width, accurately describes the exponential plasma initially, but fails as the plasma evolves. To characterize the size evolution, we fit the density transects of both Gaussian and exponential plasmas to integrals over LIF-laser-sheet thickness of the Gaussian expression (Eq. 1). The RMS radii σ_x and σ_y are ex-

tracted from the fits. Although the exponential plasma shape is not well described by the Gaussian for some time points, this function captures the size of the plasma throughout the evolution. We assume cylindrical symmetry about the x -axis for all data, $\sigma_y = \sigma_z$. Figure 5 shows the evolution of the geometric mean plasma size $\sigma_m = (\sigma_x \sigma_y \sigma_z)^{1/3} = (\sigma_x \sigma_y^2)^{1/3}$ for a Gaussian plasma with $T_e(0) = 40 \text{ K}$ and several exponential plasmas of various $T_e(0)$.

For the exponential plasmas, it is clear from the plot with unscaled axes (Fig. 5A) that smaller initial mean size and higher $T_e(0)$ leads to faster expansion. To highlight this, Fig. 5B shows the data with size scaled by the initial value and time scaled by τ_{exp} (Eq. 8), where we have set $\sigma(0)$ equal to the initial fit σ_m . In spite of the fact that the exponential plasmas lack spherical symmetry and Gaussian curvature, and thus do not satisfy the initial conditions of the self-similar expansion, this scaling causes the data to collapse to close to a universal curve over this parameter range. This is another strong indication that the expansion is predominantly hydrodynamic in nature. It also suggests a very useful phenomenological description of the plasma expansion.

Figure 5B shows that the expansion of the Gaussian plasma is well-described by the universal curve from Eq. 4. To fit the exponential data we use Eq. 4, but with a modified effective expansion time $\beta \tau_{exp}$,

$$\sigma_m(t)/\sigma_m(0) = \sqrt{1 + t^2/(\beta \tau_{exp})^2} \quad (10)$$

We find $\beta \approx 0.63$ for the range of conditions covered here, and τ_{exp} is calculated from Eq. 8 using the initial mean size $\sigma_m(0)$.

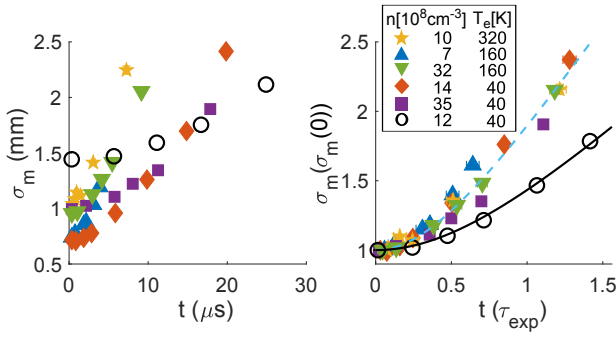


FIG. 5. Evolution of the RMS mean plasma size (σ_m) with time. Open and closed symbols correspond to Gaussian and exponential plasmas respectively. Initial peak density and electron temperature is indicated in the legend. Size and time are unscaled (left) and scaled (right) by initial size and expansion time (Eq. 8) respectively. Fit lines correspond to Eq. 10 with $\beta = 1$ (solid) and $\beta = 0.63$ (dashed).

This provides a valuable and intuitive phenomenological description of the plasma expansion. The scaling for exponential plasmas is not perfect in Fig. 5B. Plasmas with higher $T_e(0)$ and lower density expand slightly faster in scaled units. This trend is more evident if one fits the data sets for each initial condition individually independent values of β . This suggests a small influence of kinetic effects,⁴⁷ such as free-streaming, which enhances density at the expanding fronts and broadens the width of the fitted curve at each scaled time.

V. VELOCITY EVOLUTION

Figure 4(bottom) shows the x -component of the hydrodynamic velocity \vec{u} along an x -transect passing through the center of the plasma for the same data as Fig. 4(top). At all times, the Gaussian plasma displays the characteristic linear increase of the velocity with distance from the plasma center (Eq. 9) that is a hallmark of the self-similar expansion. Linearity extends essentially until the density is too low to obtain a reliable measure of velocity, beyond $r \sim 2\sigma_m(0)$, where the density is $\lesssim 10\%$ of its peak value. The velocity curve approaches $\vec{u} = r/t$ for $t \gg \beta\tau_{exp}$.

The velocity profile for the exponential plasma deviates dramatically from the prediction of the self-similar solution (Eq. 9) as shown by Fig. 4(bottom). For an exponential density profile (Eq. 2), the acceleration along the x -axis due to the electron pressure gradient is $\dot{u}_x = \text{sgn}(x)k_B T_e/m_i \alpha$. Even with smoothing of the central density peak in the initial distribution due to experimental imperfections (Fig. 2(C-D)), this form of the acceleration suggests that a steep velocity gradient should form very quickly near the plasma center, as evident in Fig. 4(bottom). Further from the center, there are extrema in the velocity after just a few microseconds. As the plasma evolves, the extrema move out, and they cause the steepening of the density gradient observed at later times in Fig. 4(top).

The hydrodynamic nature of the expansion for the exponential plasma is evident in the universality of the velocity profiles in appropriate scaled units, in analogy to the behavior

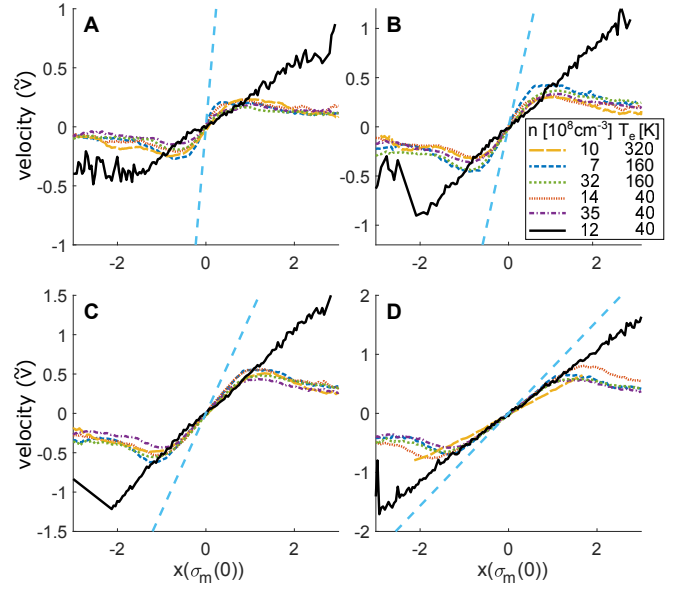


FIG. 6. Transects passing through the plasma origin along the x -axis of the x -component of the hydrodynamic velocity at $t/\beta\tau_{exp} = 0.23 \pm 0.02$ (A), 0.49 ± 0.09 (B), 0.80 ± 0.05 (C), 1.28 ± 0.35 (D). Velocity is given in units of $\tilde{v} = \sigma_m(0)/\beta\tau_{exp} = \sqrt{k_B T_e(0)/m_i}/\beta$, and position is scaled by $\sigma_m(0)$. Initial peak density and $T_e(0)$ are indicated in the legend. The long dashed line corresponds to the terminal velocity profile $\vec{u} = \vec{r}/t$. The solid line is a Gaussian plasma. All other data corresponds to exponential plasmas.

of the self-similar hydrodynamic expansion (Eqs. 4-9). Figure 6 shows the x -component of expansion velocity along the x -axis for various initial conditions at the same times in units of $\beta\tau_{exp}$. Velocity and position are scaled in units of $\sigma_m(0)/\beta\tau_{exp}$ and $\sigma_m(0)$ respectively. In scaled units, the velocity curves for exponential plasmas are universal, with deviations mostly due to spread in values of $t/\beta\tau_{exp}$ that are displayed in each subplot. The velocity extrema approach $v \approx \sqrt{k_B T_e(0)/m_i}/\beta$. At early times and near the plasma center, the density gradient, acceleration, and scaled velocity is much higher for the exponential plasmas than for Gaussian plasma. The velocity in scaled units for the Gaussian plasma uniformly and monotonically approaches the ballistic limit, as expected from Eq. 9, and eventually matches the exponential plasma in the center.

VI. TEMPERATURE EVOLUTION

While a hydrodynamic description assuming quasi-neutrality (Eq. 3) appears to capture the behavior of the exponential plasma very well, the assumption of quasi-neutrality is suspect near the plasma center. The Debye length for electrons, $\lambda_D = \sqrt{\epsilon_0 k_B T_e / n_e e^2}$ for $n_e = 10^9 \text{ cm}^{-3}$ and $T_e = 320 \text{ K}$ is $40 \mu\text{m}$, which is on the order of the length scale of the central peak, so significant non-neutrality is possible near the origin for high-temperature and low-density exponential plasmas. Figure 7 shows the evolution of the ion temperature in the center of the plasma, which displays effects likely arising

from non-neutrality.

The evolution of ion temperature for exponential plasmas for $T_e(0) = 40$ K and for the Gaussian plasma follows the expected behavior for ion equilibration after UCNP creation, which is well studied.^{26,28,39,67,68} Ions have very little initial kinetic energy because of the controlled UCNP creation process. However, there is a relatively large amount of potential energy due to electrical interactions between ions in the random spatial distribution inherited from the precursor atoms. In a time equal to the inverse of the ion plasma oscillation frequency, $1/\omega_{pi} = (e^2 n / \epsilon_0 m_i)^{-1/2} \sim 1 \mu\text{s}$, ions develop spatial correlations, and potential energy is changed into kinetic as the system equilibrates. The equilibration temperature, defined as T_{DIH} , depends on initial density and electron temperature. Assuming overall plasma neutrality, T_{DIH} can be directly found with molecular dynamics⁶⁷ or expressed in terms of analytic approximations of equilibrium correlation energy determined with molecular dynamics simulations.^{39,70} $T_{DIH} \approx e^2 / (8\pi\epsilon_0 a k_B) \sim 1$ K where $a = [3 / (4\pi n)]^{1/3}$ is the Wigner-Seitz radius. Figure 7 shows that for low $T_e(0)$, ions equilibrate with $T / T_{DIH} \sim 1$. Subsequent moderate heating on a longer timescale reflects dissipation of ion acoustic waves and^{47,50} and electron-ion energy exchange.⁶⁸

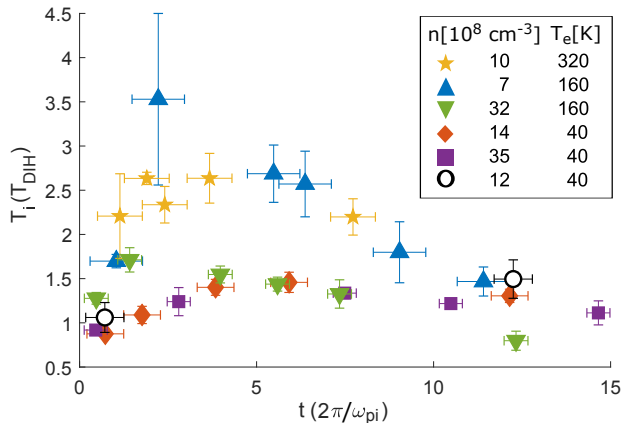


FIG. 7. Evolution of the ion temperature in the plasma center. Temperatures are scaled by the disorder-induced-heating temperature T_{DIH} and time is scaled by the ion oscillation period $2\pi/\omega_{pi}$. The Gaussian plasma equilibrates to T_{DIH} within $2\pi/\omega_{pi}$, as expected from disorder-induced heating. This is also seen with the exponential plasmas for $T_e = 40$ K. However, for the exponential plasmas with $T_e = 160, 320$ K, significant heating is seen, especially for the $T_e = 320$ K and the low density $T_e = 160$ K data, indicative of kinetic effects from a Coulomb explosion.

For $T_e(0) = 160$ K and $T_e(0) = 320$ K, and more dramatically for lower ion density, however, ions reach much higher scaled temperatures on a rapid timescale. We hypothesize that this extra heating arises from plasma non-neutrality, which introduces additional Coulomb energy in the central region and subsequent Coulomb explosion.

VII. CONCLUSION

We characterized the expansion of an UCNP with an initial exponentially decaying density distribution and compared it to the well-studied self-similar expansion of an UCNP with a Gaussian density distribution. The expansion of an exponential UCNP displays the hallmarks of hydrodynamic phenomenon and is driven by the electron pressure gradient. The characteristic length (σ_0) and time scale (τ_{exp}) that parameterize the expansion of Gaussian plasmas also provide useful scaling factors for evolution of the size and velocity distribution for exponential plasmas.

The ion temperatures display excess heating near the density peak in the exponential case for low density and high electron temperature, suggesting significant non-neutrality that might introduce dynamics similar to a Coulomb explosion in this region. Further study of this phenomena is needed.

Modeling the expansion of an exponential UCNP is an excellent target for various numerical methods, such as two-fluid models, models that consider kinetic effects, and MD simulations. It would be informative to compare the observations described here with two-component MD codes with open boundary conditions⁷¹ and recently developed tools for describing heterogeneous, non-equilibrium plasmas subject to effects of strong coupling.⁷² This would provide validation of numerical methods and additional insight into some aspects of the expansion of the exponential plasma, such as electron temperature evolution and the influence of Coulomb-explosion effects on ion temperature near the plasma center. Further study is also needed to explore the possible formation of shock waves associated with the extrema in the velocity transects and steepening of the density gradient.

ACKNOWLEDGMENTS

This material is based upon work supported by the Air Force Office of Scientific Research through Grant No. FA9550-17-1-0391 and the National Science Foundation Graduate Research Fellowship Program under Grant No. 1842494. Any opinions, findings, and conclusions or recommendations expressed in this material are those of the authors and do not necessarily reflect the views of the National Science Foundation.

DATA AVAILABILITY

The data that support the finding of this study are available from the corresponding author upon reasonable request.

¹J. T. Karpen and C. R. DeVore, *ApJ* **320**, 904 (1987).

²C. Courtois, R. A. D. Grundy, A. D. Ash, D. M. Chambers, N. C. Woolsey, R. O. Dendy, and K. G. McClements, *Phys. Plasmas* **11**, 3386 (2005).

³D. Perrone, R. O. Dendy, I. Furno, R. Sanchez, G. Zimbaro, A. Bovet, A. Fasoli, K. Gustafson, S. Perri, P. Ricci, and F. Valentini, *Space Sci. Rev.* **178**, 233 (2013).

⁴S. J. Bradshaw and J. Raymond, *Space Sci. Rev.* **178**, 271 (2013).

⁵M. J. West, S. J. Bradshaw, and P. J. Cargill, *Sol. Phys.* **252**, 89 (2008).

- ⁶E. L. Clark, K. Krushelnick, M. Zepf, F. N. Beg, M. Tatarakis, A. Machacek, M. I. K. Santala, I. Watts, P. A. Norreys, and A. E. Dangor, *Phys. Rev. Lett.* **85**, 1654 (2000).
- ⁷R. A. Snavely, M. H. Key, S. P. Hatchett, T. E. Cowan, M. Roth, T. W. Phillips, M. A. Stoyer, E. A. Henry, T. C. Sangster, M. S. Singh, S. C. Wilks, A. MacKinnon, A. Offenberger, D. M. Pennington, K. Yasuike, A. B. Langdon, B. F. Lasinski, J. Johnson, M. D. Perry, and E. M. Campbell, *Phys. Rev. Lett.* **85**, 2945 (2000).
- ⁸A. Maksimchuk, S. Gu, K. Flippo, D. Umstadter, and V. Y. Bychenkov, *Phys. Rev. Lett.* **84**, 4108 (2000).
- ⁹J. Badziak, E. Woryna, P. Parys, K. Y. Platonov, S. Jabłoński, L. Ryć, A. B. Vankov, and J. Wołowski, *Phys. Rev. Lett.* **87**, 215001 (2001).
- ¹⁰J. Fuchs, Y. Sentoku, S. Karsch, J. Cobble, P. Audebert, A. Kemp, A. Nikroo, P. Antici, E. Brambrink, A. Blazevic, E. M. Campbell, J. C. Fernández, J. Gauthier, M. Geissel, M. Hegelich, H. Pépin, H. Popescu, N. Renard-LeGalloudec, M. Roth, J. Schreiber, R. Stephens, and T. E. Cowan, *Phys. Rev. Lett.* **94**, 045004 (2005).
- ¹¹L. Romagnani, J. Fuchs, M. Borghesi, P. Antici, P. Audebert, F. Ceccherini, T. Cowan, T. Grismayer, S. Kar, A. Macchi, P. Mora, G. Pretzler, A. Schiavi, T. Toncian, and O. Willi, *Phys. Rev. Lett.* **95**, 195001 (2005).
- ¹²M. Murakami, Y.-G. Kang, K. Nishihara, S. Fujioka, and H. Nishimura, *Phys. Plasmas* **12**, 062706 (2005).
- ¹³P. Mora, *Phys. Plasmas* **12**, 112102 (2005).
- ¹⁴T. Grismayer and P. Mora, *Phys. Plasmas* **13**, 032103 (2006).
- ¹⁵D. R. Symes, M. Hohenberger, A. Henig, and T. Ditmire, *Phys. Rev. Lett.* **98**, 123401 (2007).
- ¹⁶S. Kulin, T. C. Killian, S. D. Bergeson, and S. L. Rolston, *Phys. Rev. Lett.* **85**, 318 (2000).
- ¹⁷F. Robicheaux and J. D. Hanson, *Phys. Rev. Lett.* **88**, 55002 (2002).
- ¹⁸F. Robicheaux and J. D. Hanson, *Phys. Plasmas* **10**, 2217 (2003).
- ¹⁹S. Laha, P. Gupta, C. E. Simien, H. Gao, J. Castro, and T. C. Killian, *Phys. Rev. Lett.* **99**, 155001 (2007).
- ²⁰G. M. Gorman, M. K. Warrens, S. J. Bradshaw, and T. C. Killian, (2020), arXiv:2010.16355 [physics.plasm-ph].
- ²¹T. C. Killian, S. Kulin, S. D. Bergeson, L. A. Orozco, C. Orzel, and S. L. Rolston, *Phys. Rev. Lett.* **83**, 4776 (1999).
- ²²T. C. Killian, T. Pattard, T. Pohl, and J. M. Rost, *Phys. Rep.* **449**, 77 (2007).
- ²³M. Lyon and S. L. Rolston, *Rep. Prog. Phys.* **80**, 017001 (2017).
- ²⁴H. J. Metcalf and P. van der Straten, *Laser Cooling and Trapping* (Springer-Verlag, New York, New York, 1999).
- ²⁵J. P. Morrison, C. J. Rennick, J. S. Keller, and E. R. Grant, *Phys. Rev. Lett.* **101**, 205005 (2008).
- ²⁶C. E. Simien, Y. C. Chen, P. Gupta, S. Laha, Y. N. Martinez, P. G. Mickelson, S. B. Nagel, and T. C. Killian, *Phys. Rev. Lett.* **92**, 143001 (2004).
- ²⁷F. Cornolti, F. Ceccherini, S. Betti, and F. Pegoraro, *Phys. Rev. E* **71**, 056407 (2005).
- ²⁸M. S. Murillo, *Phys. Rev. Lett.* **87**, 115003 (2001).
- ²⁹S. G. Kuzmin and T. M. O’Neil, *Phys. Plasmas* **9**, 3743 (2002).
- ³⁰S. Mazevet, L. A. Collins, and J. D. Kress, *Phys. Rev. Lett.* **88**, 55001 (2002).
- ³¹D. O. Gericke, M. S. Murillo, D. Semkat, M. Bonitz, and D. Kremp, *J. Phys. A* **36**, 6087 (2003).
- ³²M. S. Murillo, *Phys. Rev. Lett.* **96**, 165001 (2006).
- ³³M. S. Murillo, *Phys. Plasmas* **14**, 055702 (2007).
- ³⁴T. Pohl, T. Pattard, and J. M. Rost, *Phys. Rev. A* **70**, 033416 (2004).
- ³⁵T. Pohl, T. Pattard, and J. M. Rost, *Phys. Rev. Lett.* **94**, 205003 (2005).
- ³⁶Y. C. Chen, C. E. Simien, S. Laha, P. Gupta, Y. N. Martinez, P. G. Mickelson, S. B. Nagel, and T. C. Killian, *Phys. Rev. Lett.* **93**, 265003 (2004).
- ³⁷S. Laha, Y. C. Chen, P. Gupta, C. E. Simien, Y. N. Martinez, P. G. Mickelson, S. B. Nagel, and T. C. Killian, *Eur. Phys. J. D* **40**, 51 (2006).
- ³⁸G. Bannasch, J. Castro, P. McQuillen, T. Pohl, and T. C. Killian, *Phys. Rev. Lett.* **109**, 185008 (2012).
- ³⁹M. Lyon, S. D. Bergeson, and M. S. Murillo, *Phys. Rev. E* **87**, 033101 (2013).
- ⁴⁰T. S. Strickler, T. K. Langin, P. McQuillen, J. Daligault, and T. C. Killian, *Phys. Rev. X* **6**, 021021 (2016).
- ⁴¹S. Ichimaru, *Rev. of Mod. Phys.* **54**, 1017 (1982).
- ⁴²M. Lyon, S. D. Bergeson, G. Hart, and M. Murillo, *Sci. Rep.* **5**, 1 (2015).
- ⁴³M. S. Murillo, *Phys. Plasmas* **11**, 2964 (2004).
- ⁴⁴S. D. Bergeson, S. D. Baalrud, C. Leland Ellison, E. Grant, F. R. Graziani, T. C. Killian, M. S. Murillo, J. L. Roberts, and L. G. Stanton, *Phys. Plasmas* **26**, 100501 (2019).
- ⁴⁵G. M. Gorman, T. K. Langin, M. K. Warrens, D. Vrinceanu, and T. C. Killian, *Phys. Rev. A* **101**, 012710 (2020).
- ⁴⁶P. McQuillen, J. Castro, T. Strickler, S. J. Bradshaw, and T. C. Killian, *Phys. Plasmas* **20**, 043516 (2013).
- ⁴⁷P. McQuillen, J. Castro, S. J. Bradshaw, and T. C. Killian, *Phys. of Plasmas* **22**, 043514 (2015).
- ⁴⁸R. S. Fletcher, X. L. Zhang, and S. L. Rolston, *Phys. Rev. Lett.* **96**, 105003 (2006).
- ⁴⁹X. L. Zhang, R. S. Fletcher, and S. L. Rolston, *Phys. Rev. Lett.* **101**, 195002 (2008).
- ⁵⁰J. Castro, P. McQuillen, and T. C. Killian, *Phys. Rev. Lett.* **105**, 065004 (2010).
- ⁵¹B. J. Claessens, S. B. van der Geer, G. Taban, E. J. D. Vredendregt, and O. J. Luiten, *Phys. Rev. Lett.* **95**, 164801 (2005).
- ⁵²M. P. Reijnders, P. A. van Kruisbergen, G. Taban, S. B. van der Geer, P. H. A. Mutsaers, E. J. D. Vredendregt, and O. J. Luiten, *Phys. Rev. Lett.* **102**, 034802 (2009).
- ⁵³A. J. McCulloch, D. V. Sheludko, S. D. Saliba, S. C. Bell, M. Junker, K. A. Nugent, and R. E. Scholten, *Nature Physics* **7**, 1 (2011).
- ⁵⁴J. J. McClelland, A. V. Steele, B. Knuffman, K. A. Twedt, A. Schwarzkopf, and T. M. Wilson, *Appl. Phys. Rev.* **3**, 011302 (2016).
- ⁵⁵J. G. Franssen, J. M. Kromwijk, E. J. Vredendregt, and O. J. Luiten, “Energy spread of ultracold electron bunches extracted from a laser cooled gas,” *J. Phys. B* **51**, 035007 (2018).
- ⁵⁶J. G. H. Franssen, T. C. H. de Raadt, M. A. W. van Nijnhuijs, and O. J. Luiten, *Phys. Rev. Accel. Beams* **22**, 023401 (2019).
- ⁵⁷H. Sadeghi and E. R. Grant, *Phys. Rev. A* **86**, 052701 (2012).
- ⁵⁸R. Haenel, M. Schulz-Weiling, J. Sous, H. Sadeghi, M. Aghigh, L. Melo, J. S. Keller, and E. R. Grant, *Phys. Rev. A* **96**, 023613 (2017).
- ⁵⁹T. K. Langin, G. M. Gorman, and T. C. Killian, *Science* **363**, 61–64 (2019).
- ⁶⁰P. Mansbach and J. Keck, *Phys. Rev.* **181**, 275 (1969).
- ⁶¹T. C. Killian, M. J. Lim, S. Kulin, R. Dumke, S. D. Bergeson, and S. L. Rolston, *Phys. Rev. Lett.* **86**, 3759 (2001).
- ⁶²P. Gupta, S. Laha, C. E. Simien, H. Gao, J. Castro, T. C. Killian, and T. Pohl, *Phys. Rev. Lett.* **99**, 75005 (2007).
- ⁶³M. D. Perry and G. Mourou, *Science* **264**, 917 (1994).
- ⁶⁴E. L. Raab, M. Prentiss, A. Cable, S. Chu, and D. E. Pritchard, *Phys. Rev. Lett.* **59**, 2631 (1987).
- ⁶⁵S. B. Nagel, C. E. Simien, S. Laha, P. Gupta, V. S. Ashoka, and T. C. Killian, *Phys. Rev. A* **67**, 011401(R) (2003).
- ⁶⁶J. Castro, H. Gao, and T. C. Killian, *Plasma Phys. Control. Fusion* **50**, 124011 (2008).
- ⁶⁷T. K. Langin, T. Strickler, N. Maksimovic, P. McQuillen, T. Pohl, D. Vrinceanu, and T. C. Killian, *Phys. Rev. E* **93**, 023201 (2016).
- ⁶⁸P. McQuillen, T. Strickler, T. Langin, and T. C. Killian, *Phys. Plasmas* **22**, 033513 (2015), 1501.0694.
- ⁶⁹T. Pohl, D. Vrinceanu, and H. R. Sadeghpour, *Phys. Rev. Lett.* **100**, 223201 (2008).
- ⁷⁰S. Hamaguchi, R. T. Farouki, and D. H. E. Dubin, *Phys. Rev. E* **56**, 4671 (1997).
- ⁷¹E. V. Vikhrov, S. Y. Bronin, A. B. Klayrfield, B. B. Zelener, and B. V. Zelener, *Phys. Plasmas* **27**, 120702 (2020).
- ⁷²V. S. Dharodi and M. S. Murillo, *Phys. Rev. E* **101**, 023207 (2020).